

Re–Os Isotopic Age of the Hongqiling Cu–Ni Sulfide Deposit in Jilin Province, NE China and its Geological Significance

Han Chun-Ming^{1*}, Xiao Wen-Jiao¹, Zhao Guo-Chun², Su Ben-Xun¹, Ao Song-Jian¹, Zhang Ji-En¹, Wan Bo¹, and Zhang Zhi-Yong¹

¹Institute of Geology and Geophysics, Chinese Academy of Sciences, Beijing 100029, China

²Department of Earth Sciences, The University of Hong Kong, Pokfulam Road, Hong Kong, China

*Corresponding author: Han Chun-ming, Institute of Geology and Geophysics, Chinese Academy of Sciences, Beijing 100029, China, Tel: 8610 62007917; Fax: 86 10 62010846; E-mail: cm-han@mail.iggcas.ac.cn

Rec date: Feb 23, 2014, Acc date: Mar 06, 2014, Pub date: Mar 14, 2014

Copyright: © 2014 Han CM, et al. This is an open-access article distributed under the terms of the Creative Commons Attribution License, which permits unrestricted use, distribution, and reproduction in any medium, provided the original author and source are credited.

Abstract

The major Hongqiling Cu–Ni sulfide deposit in central Jilin Province is located in the eastern part of the Central Asian Orogenic Belt. Rhenium and osmium isotopes in sulfide minerals from the deposit have been used to determine the timing of mineralization and the source of osmium and, by inference, the ore metals. Sulfide ore samples have osmium and rhenium concentrations of 0.28–1.07ppb and 2.39–13.17ppb, respectively. Ten sulfide analyses yield an isochron age of 223 ± 9 Ma, indicating that the Cu–Ni sulfide mineralization formed in the Early Triassic. The initial $^{187}\text{Os}/^{188}\text{Os}$ ratio is 0.295 ± 0.019 (MSWD = 1.14). This data indicates that the mineralization was derived mainly from a mantle source with some quantities of crustal components introduced into the rock-forming and ore-forming systems during mineralization and magmatic emplacement.

Together with the widespread occurrence of late Carboniferous–Permian mafic–ultramafic complexes and associated Permian Cu–Ni deposits in the western part of the Central Asian Orogenic Belt (Northern Xinjiang), we conclude that mantle–crustal interactions were active during the accretion–collisional processes that led to the Cu–Ni mineralization and considerable continental growth in the late Carboniferous–Permian to mid–Triassic.

Keywords: Re–Os isotopic dating; Cu–Ni deposit; Geodynamic process; Hongqiling; NE China

Introduction

The complicated orogenic processes of the Central Asian Orogenic Belt (CAOB), characterized by considerable Phanerozoic continental growth and mantle–crust interaction, generated the Central Asian Metallogenic Domain with world-class ore deposits [1–10]. However, the connections between orogenic processes, continental growth, mantle–crust interaction and ore deposit formation unsolved. The main controversy is with regard to the timing of these geodynamic processes. Different groups of researchers have considered that orogeny ended either in the early Paleozoic [11], the Devonian–Carboniferous [12], or even late Permian to middle Triassic [7–8]. However, it is commonly accepted that the major continental growth and large-scale mineralization were in the late Carboniferous–Permian to early Mesozoic [2,13]. Therefore the relationships between these various geodynamic processes require further study.

In this study, we present new Re–Os isotopic data on Cu–Ni-bearing sulfide ores from the Hongqiling intrusion in the eastern part of the Central Asian Orogenic Belt to constrain the timing of mineralization, and to further discuss the issues raised above. The new data provide important insights into understanding of the mineralization processes and geodynamic setting of the Hongqiling Cu–Ni ore deposit in NE China.

Geological Background

The study area is situated in central Jilin Province, NE China, representing the eastern extension of the Central Asian Orogenic Belt (CAOB), developed between the North Craton to the south and the Siberia Craton to the north (Figure 1). This pair of NE China is divided into three blocks [3,5,14–16]; the Xing'an Block in the northwest, Songliao Block in the middle, and Jiamusi Block in the southeast, which are separated by the Mudanjiang and Nenjiang Faults, respectively (Figure 1).

The Songliao Block consists of Paleozoic to Mesozoic accreted arc complexes, the Mesozoic to Cenozoic Songliao Basin and Mesozoic granites that make up the Zhangguangcai Range (Figure 1) [7]. Local amphibolite facies metamorphic rocks have been identified, including the Dongfengshan Group in the north and the Hulan Group in the south [7,17,18]. However, Phanerozoic granites occupy the majority of the block. The Songliao Basin formed in the late Mesozoic over a basement of Phanerozoic granites and Palaeozoic strata [7]. The Hulan Group mainly crops out in the Hongqiling–Piaohechun area, and is composed predominantly of mica schist, gneiss, amphibolite and marble which were interpreted as the final products related to the closure of the Paleo-Asian Ocean [7,19,20].

The late Paleozoic strata are distributed mainly in the Panshi area and consist of sandstone, siltstone, shale, mudstone and carbonate, indicating a shallow marine sedimentary environment. However, it should be pointed out that the environment changed from an oceanic to an arc setting in the Late Permian with the development of intermediate-acid volcanic rocks, including andesite and rhyolite [7].

In NE China, more than 1000 mafic–ultramafic complexes have been identified [3], some of which are characterized by Cu and Ni mineralization, especially in the Hongqiling and Piaohechuan complexes (Figures 1 and 2a). Most of the important magmatic Cu–Ni sulfide deposits are developed in the Songliao Block, including those at the Hongqiling, Piaohechuan, Changren, Zhangxiang, Chajianling, Erdaogou, Sandaogang and Sanmen deposits (Figure 1; Table.1), only the Wuxing Cu–Ni deposit is located in the Jiamusi Block, of which the most representative and largest is the Hongqiling Cu–Ni deposit.

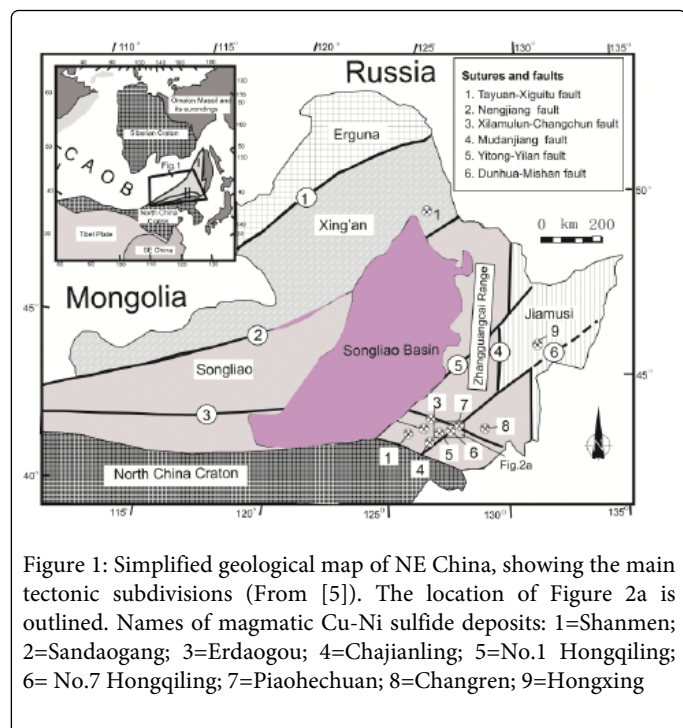


Figure 1: Simplified geological map of NE China, showing the main tectonic subdivisions (From [5]). The location of Figure 2a is outlined. Names of magmatic Cu–Ni sulfide deposits: 1=Shanmen; 2=Sandaogang; 3=Erdaogou; 4=Chajianling; 5=No.1 Hongqiling; 6= No.7 Hongqiling; 7=Piaohechuan; 8=Changren; 9=Hongxing

Geology of the Hongqiling Area

Located 38 km east-southeast of Panshi city, central Jilin Province, the Hongqiling copper-nickel deposit is the largest and economically most important deposit in the eastern CAOB, with explored reserves of 271,720 tons of Ni and 6,9940 tons of Cu [21]. The ore deposit was discovered in 1958 and exploited during the period of 1959-1961, with the construction of the present-operating mine commencing in 1964. Since the discovery of the deposit, numerous studies have been carried out on its mineralization and the host mafic-ultramafic rocks [4,22-24].

The host rocks of the Hongqiling Cu–Ni deposit are hosted by metamorphic rocks of the Lower Paleozoic Hulan Group (Figure 2a), which consists predominantly of garnet mica gneiss, biotite gneiss, amphibolite, muscovite schist, all of which show strong ductile deformation. Five mafic-ultramafic intrusions distributed in the Hongqiling deposit mining district, of which two intrusions (Nos. 1 and 7) in the southern part of the deposit area (Figure 2b) are well differentiated and zoned, and have Cu–Ni mineralization [21].

The No. 1 intrusion is 980 m long and up to 270 m wide. It extends as much as 576 m down-dip and, on the surface outcrop occupies an area of ~0.20 km² (Figure 3a). In plan view, the intrusion is an irregular lens in shape, but in vertical cross-section, the intrusion is a funnel-shaped body and become vein-like at depth (Figure 3a). The

No. 1 intrusion intrudes the Hulan Group and contains four intrusive units with the following rock types from the base upwards [4,23]: olivine websterite (4%) and lherzolite (89%) in the lower part, pyroxenite (6%) and gabbro (1%) in the upper part. The nature of the contacts between the different units is unclear in the field [4].

The No. 7 intrusion is located 10km southeast of Hongqiling town (Figure 2b). Its long axis strikes 300° and dips at 75-80° to NE (Figure 3b). It is 700m in length, and has an average width of 35m, a maximum extension of about 600 m, and a surface outcrop of ~0.013 km² [4,23]. The intrusive units include orthopyroxenite (96%), and minor norite and peridotite [4,23].

Geology of the Ore Deposit

As stated above, the Hongqiling Cu–Ni deposit consists of the No.1 and No.7 orebodies. Cu–Ni sulfide ores are hosted in the olivine websterite unit and the No. 1 orebody contains 15,200 t of Cu and 71,600 t of Ni, based upon average ore grades of 0.54% Ni and 0.11% Cu [21]. The No.7 orebody is hosted in the orthopyroxenite, norite and peridotite units and contains 204,000 t of Ni and 39,000 t of Cu, based upon the average ore grades of 2.30% Ni and 0.63% Cu [21]. In addition, 3,100 t of Co may be recovered as by-products [21].

Mineralogically, the ore minerals of the Hongqiling Cu–Ni deposit are dominantly pyrrhotite, pentlandite, chalcopyrite, violarite, pyrite, vallerite, millerite, nickeline, ilmenite, galena and magnetite, and the gangue minerals are olivine, pyroxene, plagioclase, hornblende, biotite, chlorite and serpentine.

The textures of the ore minerals include euhedral, subhedral, anhedral, subhedral-anhedral, gabbroic, poikilitic, reaction rim, sideronitic, interstitial and corrosion textures, and the ore structures are mainly massive, disseminated, sparsely disseminated, spotted and banded.

Based on cross-cutting relationships between minerals and mineral assemblages, mineralization in the Hongqiling orebody can be subdivided into the following three stages (Figure 4). The first is the magmatic crystallization stage, characterized by disseminated and massive ores with pentlandite+violarite+millerite+magnetite. The second is the auto-metamorphic stage that is characterized by the formation of massive and vein-like high grade Cu and Ni ores, and forming Cu- and Ni-bearing minerals, represented by chalcopyrite and pyrrhotite. The third is the magmatic–hydrothermal stage that is characterized mainly by chlorite and carbonate alteration, forming the carbonate+pyrite+chalcopyrite assemblage that occurs as veins.

Wall–rock alteration related to mineralization in the Hongqiling Cu–Ni ore deposit includes chloritization, carbonatization, serpentinization, talcization, uralitization, sericitization, tremolitization [23]. Characteristic minerals in the alteration zones are talc, chlorite, serpentine, sericite and carbonate.

Analytical Techniques

We collected ten samples from the Hongqiling deposit for Re–Os dating, all from fresh open-pit mining faces. To make the samples more representative, we chose samples from different ore types, including disseminated (samples HQL-1,4,5,7,9) and massive Cu–Ni ores (samples HQL-2,3,6,8,10). Variable chalcopyrite-pyrrhotite-pentlandite percentages in the samples provide a range of Re/Os ratios, since chalcopyrite-rich assemblages tend to have higher Re/Os ratios than those of the pyrrhotite-rich assemblages [25,26]. The relatively

large range of Re/Os ratio is an important factor for obtaining precise Re-Os isochron ages [26].

Name of deposit	Intrusion size (length×width) km	Mineralized rock	Orebody shape	Ore minerals	Ore structures	Reserves (1000 t) @ grade %	Data sources
Shanmen 124°28'00"E, 43°09'00"N	0.7×0.29	Pyroxenite	Bedded	Pyrrhotite, chalcocopyrite, pentlandite	Sparse disseminated	Cu: 0.04-0.38%, Ni: 0.34-0.40%	[48]
Erdaogou 127°09'57"E, 43°12'15"N	1.44×0.07	Ol-pyroxenite, Pl- pyroxenite		Pyrrhotite, pentlandite, chalcocopyrite, violarite, pyrite	Disseminated, spotted	Cu:1.55 @0.04-0.38%, Ni:4.67@ 0.34-0.40%	[21]
Sandaogang 127°09'57"E, 43°12'15"N	0.47×0.008	pyroxenolite Hb- pyroxenolite	vein-shaped	Pyrrhotite, pentlandite, chalcocopyrite	Sparse disseminated, massive	Cu:@0.26-0.48%, Ni:@ 0.68-0.74%	[48]
Chajianling 126°21'00"E, 42°52'00"N	0.10	Pyroxene -amphibolite, Hb- pyroxenolite	lens-shaped	Pyrrhotite, pentlandite, chalcocopyrite	Massive	Cu:@0.14%, Ni:@ 0.30-0.65%	[48]
No.1 of Hongqiling 126°25'02"E, 42°53'10"N	0.98×0.20	pyroxenolite, Ol- pyroxenolite, Pyroxene -peridotite	Bedded, vein, lens, sack-like	Pyrrhotite, pentlandite, chalcocopyrite, pyrite	Sparse disseminated, massive	Ni: 71.62@0.54%, Cu:15.21@ 0.11%	[23]
No.7 of Hongqiling 126°44'40"E, 42°59'30"N	0.75×0.03	Orthopyroxenite, Pyroxene -peridotite	Bedded, vein, lens, sack-like	Pyrrhotite, pentlandite, chalcocopyrite, violarite, pyrite	Dense disseminated, massive	Ni: 200.10@2.30%, Cu:54.73@ 0.63% Co:0.31@ 0.05%	[4]
Piaohechuan 127°22'10"E, 43°15'50"N	0.63×0.20	Pl- Hb –Ol-pyroxenite	Vein, lens-shaped	Pyrrhotite, pentlandite, chalcocopyrite, pyrite	Disseminated, spotted, massive	Ni:10.56@ 0.12-1.04%, Cu:3.94@ 0.05-0.39%,	[48]
Changren 128°57'11"E, 42°49'44"N	0.33	Pyroxene -peridotite	Bedded, veined	Pyrrhotite, pentlandite, chalcocopyrite	Disseminated, spotted, massive	Ni: 18.9@ 0.44%, Cu:6.6@ 0.15%,	[48]
Wuxing 126°16'00"E, 43°09'00"N	4.7×1.7	Diopside	Bedded , lens-shaped	Pyrrhotite, pentlandite, chalcocopyrite, merenskyite, pyrite	Massive, disseminated	Ni: 8.63@ ?%, Cu:14.88 0.20%,	[48]

Table 1: Summary of basic characteristics of major Cu-Ni- (PGE) deposits in the Northeastern China. Ol=olivine; Hb=hornblende; Pl=plagioclase

Re-Os isotopic analyses were performed at the National Research Center of Geoanalysis. The details of the chemical procedure are described by [27-29], and are briefly summarized as follows.

The carius tube (a thick-walled borosilicate glass ampoule) digestion technique was used. The weighed sample was loaded in a carius tube through a long thin-neck funnel. The mixed 190Os and 185Re spike solution and 2 ml of 10 N HCl and 6 ml of 16 N HNO3 were added while the bottom part of the tube was frozen at -80 to - in

an ethanol-liquid nitrogen slush; the top was sealed using an oxygen-propane torch. The tube was then placed in a stainless-steel jacket and heated for 10 h at 230°C. Upon cooling, the bottom part of the tube was kept frozen, the neck of the tube was broken, and the contents of the tube were poured into a distillation flask and the residue was washed out with 40 ml of water.

Separation of osmium by distillation and separation of rhenium by extraction was performed based on the analytical method from [30]. A

TJA PQ-EXCELL ICP-MS was used for the determination of the Re and Os isotope ratio.

Average blanks for the total carius tube procedure were ca. 10 pg Re and ca. 1 pg Os. The analytical reliability was tested by repeated analyses of molybdenite standard HLP-5 from a carbonate vein-type molybdenum-lead deposit in the Jinduicheng-Huanglongpu area of Shaanxi Province, China. Fifteen samples were analyzed over a period of 5 months. The uncertainty in each individual age determination was about 0.35% including the uncertainty of the decay constant of ^{187}Re , uncertainty in isotope ratio measurement, and spike calibrations. The average Re-Os age for HLP-5 is 221.3 ± 0.3 Ma (95% confidence limit) [31]. Median age and mean absolute deviation were 221.34 ± 0.12 Ma. The average Re concentration was 283.71 ± 1.54 $\mu\text{g/g}$. The average Os concentration was 657.95 ± 4.74 ng/g.

demonstrate relatively large variations. For massive Cu-Ni ores (samples HQL-2, 3, 6, 8, 10), the total Re and Os contents range from 83.78 ± 0.66 to 236.60 ± 2.10 ppb and 0.2899 ± 0.0030 to 1.067 ± 0.014 ppb, respectively, whereas for the disseminated ores (samples HQL-1, 4, 5, 7, 9), the Re and Os contents vary from 93.17 ± 0.7 to 134.7 ± 1.2 ppb and 0.318 ± 0.006 to 0.5200 ± 0.0187 ppb, respectively. A regression analysis was applied to the ten analytical data and yielded an isochron age of 222.9 ± 9.1 Ma, with initial $^{187}\text{Re}/^{188}\text{Os}$ ratio of 0.295 ± 0.019 and a mean square of weighted deviation (MSWD) of 1.141 (Figure 5). The isochron age was calculated by means of the ^{187}Re decay constant of 1.666×10^{-11} /year [32] using the ISOPLOT software (Model 3) [33]. This isochron age can reflect the ore-forming age of the Hongqiling Cu-Ni deposit.

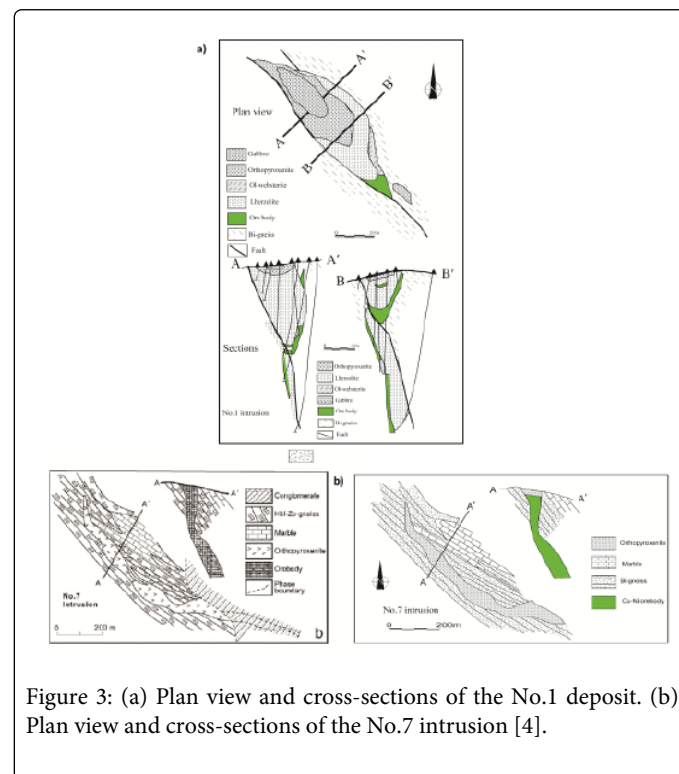
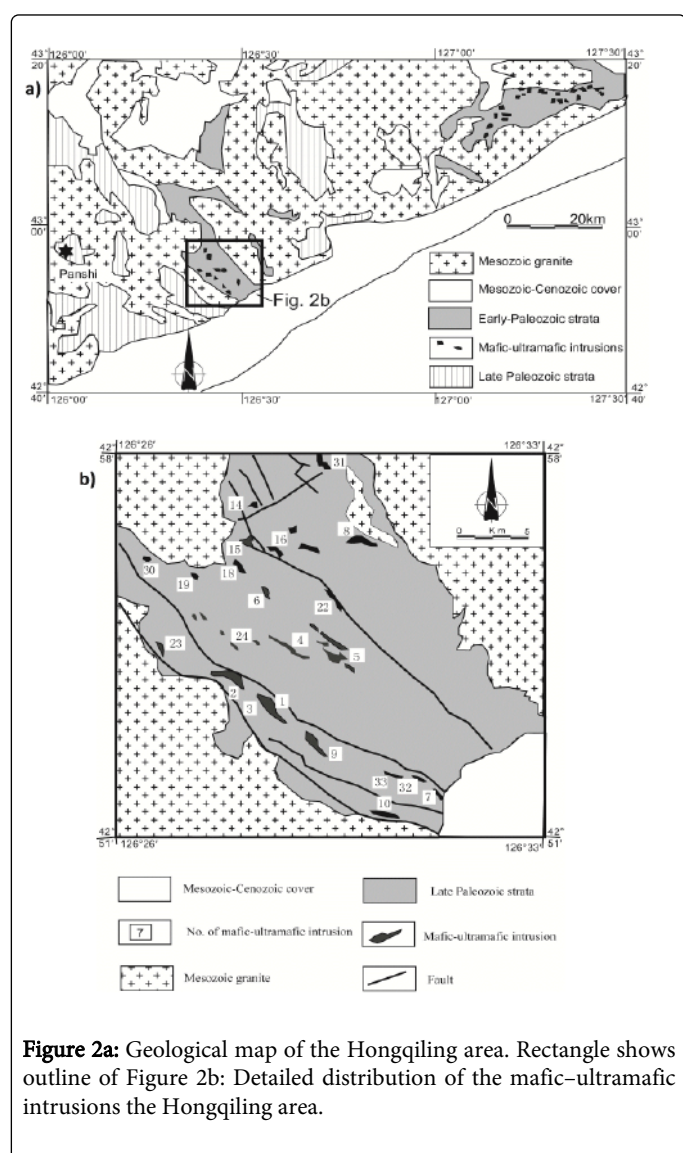


Figure 3: (a) Plan view and cross-sections of the No.1 deposit. (b) Plan view and cross-sections of the No.7 intrusion [4].

Discussion

Initial $^{187}\text{Os}/^{188}\text{Os}$ and source of ore-forming metals

The Re–Os isotope system has been recognized as a geochemical tool not only for directly dating mineralization but also for defining the ore forming process of Cu-Ni sulfide deposits, and thus is a powerful tracer of sulfide ore formation and can be a highly sensitive monitor of the extent of crustal involvement during ore genesis [25]. Since the initial $^{187}\text{Os}/^{188}\text{Os}$ ratios of the crust (0.2–10) are higher than those of the mantle (0.11–0.15) [34], $^{187}\text{Os}/^{188}\text{Os}$ ratios can be used to readily discern different sources [35].

The Hongqiling Cu-Ni sulfides ores possess an initial $^{187}\text{Os}/^{188}\text{Os}$ ratio of 0.295 ± 0.019 (Figure 5), which is considerably greater than chondritic value as well as those of the mantle at 222.9 Ma, indicating that crustal components were involved in the Os source of the Hongqiling ores.

Analytical Result

The abundance of Re and Os and the osmium isotopic compositions of the Cu-Ni sulfide ores from the Hongqiling mine are shown in Table 2. Due to different ore types, the Re and Os contents

In order to describe the Os isotopic composition at a given time, a parameter of γ_{Os} was introduced by Walker et al. [36,37].

$$\gamma_{Os} (T) = 100 \left[\frac{^{187}Os/^{186}Os}{^{187}Os/^{186}Os} \right]_{\text{sample}} (T) / \left[\frac{^{187}Os/^{186}Os}{^{187}Os/^{186}Os} \right]_{\text{chondrite}} (T) - 1$$

Owing to high Re/Os ratios in the crust, γ_{Os} will have a large positive value with increasing crustal material entering the magmatic or ore-forming systems, and, by contrast, Re-loss in the systems can cause negative γ_{Os} [38]. According to the formula of [36], and with a decay constant of 1.666×10^{-11} /year [32], the γ_{Os} values for the Hongqiling Cu-Ni sulfide ores were calculated based on the isochron age of 222.9 ± 9.1 Ma and their corresponding initial $^{187}Os/^{188}Os$ ratios. Table 3 shows that the γ_{Os} values for the Hongqiling Cu-Ni sulfide ores range from 119.32 to 142.35. The initial $^{187}Os/^{188}Os$ ratio of 0.295 ± 0.019 for the Hongqiling sulfides is higher than that of 0.1089 ± 0.00035 reported for the uncontaminated Archean komatite-related Cu-Ni sulfide ores [39]. These data reflect that mafic-ultramafic magmas were mixed with crustal components during the uprise of the magma or within magma chambers in the crust. This process is analogous to the crustal contamination of the Voisey's Bay magma by the Tasiuyak paragneiss where siderophile and chalcophile elements were selectively incorporated [40] and the case of the Jinbulake intrusion in Xinjiang where crustal sulfides were selectively incorporated to magmas [41]. Such features can also be seen in the common Os vs. Re/Os diagram (Figure 6).

Age of mineralization and its geodynamic significance

Ten sulfide samples yielded a Re-Os isochron age of 222.9 ± 9.1 Ma (2σ), as shown on the $^{187}Os/^{188}Os$ versus $^{187}Re/^{188}Os$ plot (Figure 5). Six pyrrhotite samples separated from massive Ni-Cu sulfide ores of the Fujia (No. 7) deposit yielded a Re-Os isotopic isochron age of 208 ± 21 Ma [42]. SHRIMP U-Pb zircon analyses on a leucogabbro and plagioclase-bearing pyroxenite of the Hongqiling and Piaohechuan complexes yielded weighted mean ^{206}Pb - ^{238}U ages of 216 ± 5 Ma and 217 ± 3 Ma, respectively [43]. Taken together, these data suggest that the mafic-ultramafic intrusions were emplaced at 216-217 Ma, the main Cu-Ni mineralization occurred at 208-222 Ma [4].

In the Middle Triassic, large scale magmatism and Cu-Ni mineralization in NE China may have been triggered by the re-melting of Paleozoic accretion-collision complexes and older continental margins [44], possibly resulted from the delamination of the subcontinental lithospheric mantle, which caused the upwelling of asthenospheric mantle and partial melting of the overlying lithospheric mantle [42,45]. It is suggested that a significant amount of crustal contamination during magmatic crystallization is not a necessary condition for the formation of the Cu-Ni sulfide deposits, although the presence of marble xenoliths decarbonized to diopside-rich skarns and of high CaO/SiO₂ in the Jinchuan intrusion does indicate appreciable carbonate contamination, and the assimilation of the carbonate-rich fluids increased the oxygen fugacity of the magma, which led to the segregation of the Cu-Ni sulfides [46]. Since the Cu-Ni sulfides occur exclusively at the base of the associated igneous bodies in the studied complexes, we suggest dense sulfide and olivine were carried along in rapidly flowing magma in the narrow parts of conduits feeding the intrusion, and where these conduits widened out on entering the main body [42]. Similar processes have been proposed elsewhere, such as in the Jinchuan and Kalatongke Cu-Ni deposits [47].

Minerals	Stage 1	Stage 2	Stage 3
Olivine	=====		
Eusterite	=====		
Clinopyroxene	=====		
Hornblende	=====		
Biotite	=====		
Labradorite	=====		
Pentlandite	=====		
Violarite	=====		
Millerite	=====		
Chalcocopyrite		=====	=====
Pyrite		=====	=====
Pyrrhotite		=====	=====
Tremolite		=====	
Talc		=====	
Saponite		=====	
Serpentine		=====	
Chlorite			=====
Carbonate			=====
Sericite			=====
Magnetite	=====		

Figure 4: Paragenetic sequence of minerals in the Hongqiling Cu-Ni deposit.

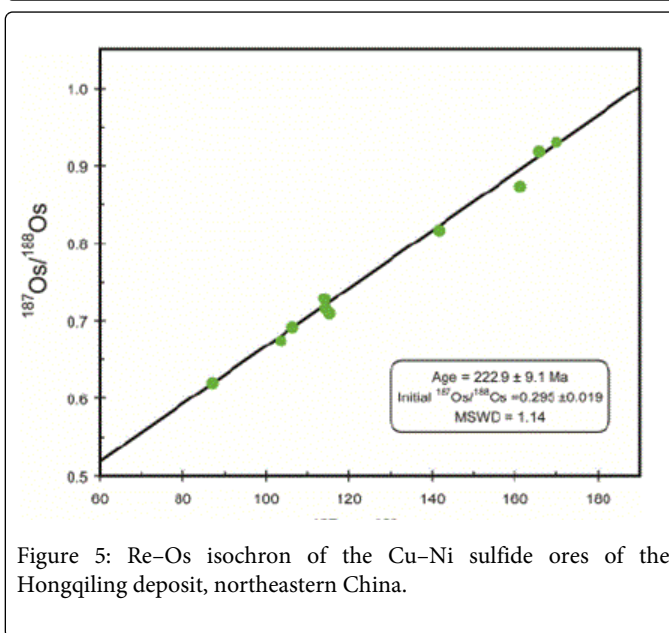


Figure 5: Re-Os isochron of the Cu-Ni sulfide ores of the Hongqiling deposit, northeastern China.

Therefore we conclude that crust contamination was active during the accretion-collision processes that led to the Cu-Ni mineralization and considerable continental growth in the late Carboniferous-Permian to mid-Triassic. U-Pb isotopic analysis of detrital zircons from a kyanite-garnet schist of the Hulan Group indicate a maximum deposition age of 287 ± 6 Ma, and Rb-Sr mineral isochron ages indicate that metamorphism occurred at ~ 250 Ma for the Hulan Group [5] (Table 3). The field geological, petrological and geochemical signatures of these rocks of the Fulan Group show they are related to the final closure of the Paleo-Asian Ocean [7]. Thus the final closure time has been put as late as Triassic. This is in good agreement with the regional tectonic analysis which also suggests that the termination time of the Central Asian Orogenic Belt was in the end-Permian to mid-Triassic [8] (Figure 7). This is consistent with the fact that new

SHRIMP and LA-ICP-MS U-Pb zircon data from para- and orthogneisses and granitoids confirm the latest Triassic-Early Jurassic termination of the eastern Central Asian Orogenic Belt, the development of which was transferred to the Pacific tectonic domain [48,49].

Conclusions

The Hongqiling magmatic Cu-Ni sulfide ore deposit in the eastern part of the Central Asian Orogenic Belt Orogenic Belt has a Re–Os isochron age of 223 ± 9 Ma. The sulfide ores possess an initial $^{187}\text{Os}/^{188}\text{Os}$

^{188}Os ratio of 0.295 ± 0.019 , and γOs values of 119.32–142.35, reflecting a result of significant crustal contamination to the metal-rich magmatic system.

The major Cu–Ni orebodies of the Hongqiling deposit were hosted in mafic–ultramafic intrusions which are considered to have formed by the accretional-collisional processes of the Central Asian Orogenic Belt (CAOB), possibly resulting from the delamination of the subcontinental lithospheric mantle, causing the upwelling of asthenospheric mantle and partial melting of overlying lithospheric mantle in the Middle Triassic.

Sample number	Ore type	Sample weight (g)	Re(ppb) (2σ) ^a	Common Os (ppb)(2σ) ^a	Os (ppb) (2σ)	Re/Os	$^{187}\text{Re}/^{188}\text{Os}$ (2σ)	$^{187}\text{Os}/^{188}\text{Os}$ (2σ) ^b	$^{187}\text{Os}/^{188}\text{Os}$ (i)	γOs
HQL-1	Disseminated	0.307	106.8(0.8)	3.652(0.029)	0.3886(0.006)	29.24	141.3(1.6)	0.8179(0.0110)	0.2921	132.74
HQL-2	Massive	0.331	138.8(1.0)	6.310(0.053)	0.5701(0.007)	22.00	106.2 (1.2)	0.6942(0.0082)	0.2990	138.24
HQL-3	Massive	0.205	236.6(2.1)	13.17(0.17)	1.067(0.014)	17.97	86.75(1.34)	0.6223(0.0093)	0.2995	138.62
HQL-4	Disseminated	0.302	116.2(0.9)	4.906(0.059)	0.4566(0.006)	23.69	114.4(1.7)	0.7151(0.0102)	0.2894	130.59
HQL-5	Disseminated	0.309	93.17(0.7)	2.793(0.044)	0.3180(0.006)	33.36	161.2(2.8)	0.8751(0.0186)	0.2753	119.32
HQL-6	Massive	0.400	131.5(2.1)	5.569(0.114)	0.5208(0.0103)	23.61	114.1(3.0)	0.7186(0.0191)	0.2940	134.26
HQL-7	Disseminated	0.300	113.9(1.0)	5.319(0.094)	0.4664(0.0064)	21.41	103.4(2.0)	0.6739(0.0134)	0.2892	130.37
HQL-8	Massive	0.316	83.78(0.66)	2.392(0.022)	0.2899(0.0030)	35.03	169.2(2.0)	0.9316(0.0088)	0.3020	140.62
HQL-9	Disseminated	0.405	134.7(1.2)	5.650(0.228)	0.5200(0.0187)	23.84	115.1(4.8)	0.7073(0.0375)	0.2790	122.30
HQL-10	Massive	0.302	91.84(0.73)	2.680(0.047)	0.3209(0.0059)	34.27	165.5(3.2)	0.9200(0.0213)	0.3042	142.35

Table 2: Re–Os isotope data for the Cu–Ni sulfide ores from the Hongqiling deposit.

(1) Os in Re/Os is common Os. Common Os and common ^{187}Os are calculated according to the Nier value. (2) The calculation formula

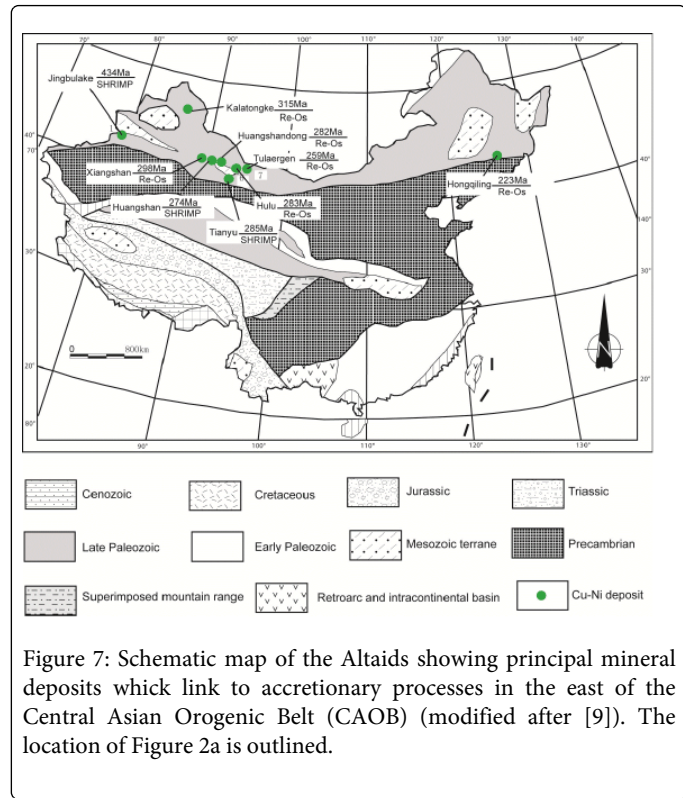
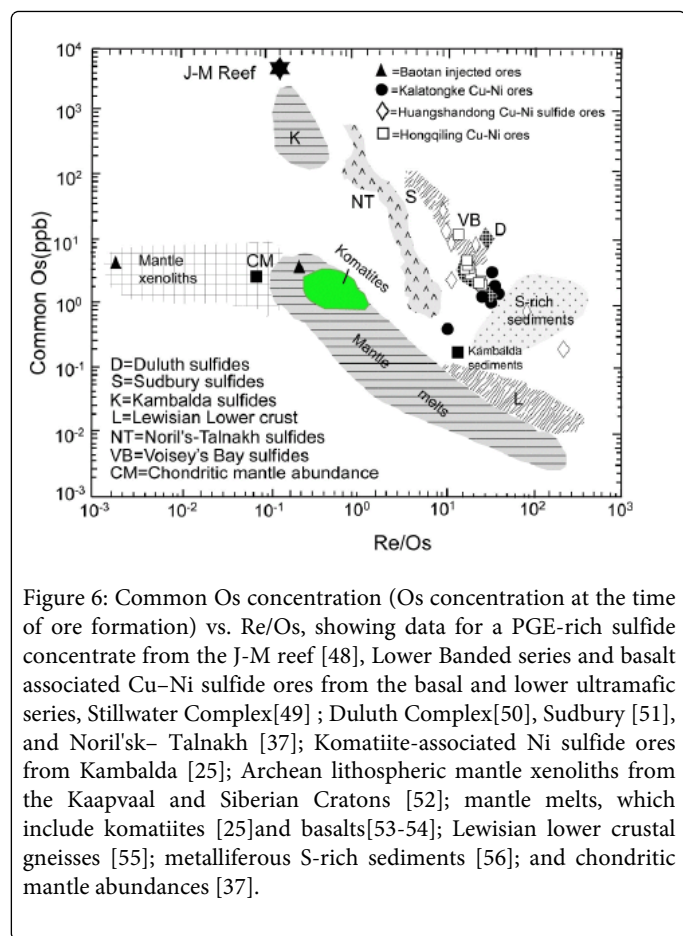
$$\text{isyOs} = 100 \left[\frac{(^{187}\text{Os}/^{188}\text{Os})_{\text{sample}}(T) / (^{187}\text{Os}/^{188}\text{Os})_{\text{chondrite}}(T) - 1}{\text{where } (^{187}\text{Os}/^{188}\text{Os})_{\text{chondrite}} = 0.09531 + 0.40186(e^{\lambda\text{Re}^*t} - 4.558E9 - e^{\lambda\text{Re}^*t})} \right] = 0.125519$$
 at 222.9Ma, using the ^{187}Re decay constant $\lambda = 1.666 \times 10^{-11}$ /year; aRe and Os uncertainty <1% at 2 standard errors of the mean, including error samples and spike weighting, spike calibration, mass spectrometric analysis, fractionation correction and measured isotope ratios in the samples. b $^{187}\text{Os}/^{188}\text{Os}$ uncertainty <1% at 2 standard errors of the mean, including error in mass spectrographic analysis, fractionation correction and measured isotope ratios in the samples.

Acknowledgements

We are indebted to Bin Cui, Kezhang Qin, Lianchang Zhang, Tianlin Ma, Zhiliang Wang, and Jianming Yang for thoughtful discussions. Many of the ideas in this paper were initiated and rectified during these discussions. We are grateful to S.A. Wilde and B.F. Windley for their constructive discussions and comments on an early version of the manuscript, which led to substantial improvements to the paper. The authors wish to thank Holly Stein and a anonymous reviewers for their useful comments on the manuscript and Andy Whitham for his editorial assistance. This study was financially supported by funds from the NSFC Projects (41272107 and 40973036), and the State 305 project (2011BAB06B04-01). This paper is a contribution to the ILP (ERAS) and IGCP 480.

Name of deposits	of Dated minerals/rocks	Dating methods	Ages/ (Ma)	Data sources
Hongqiling	Biotite	40Ar-39Ar isochron	225 ± 0.9	[24]
..	Amphibole	40Ar-39Ar isochron	246 ± 5.7	[24]
..	Amphibole	40Ar-39Ar isochron	250.07 ± 2.44	[24]
..	Gabbro	SHRIMP zircon U-Pb	216 ± 5	[4]
Piaohechuan	Gabbro	SHRIMP zircon U-Pb	217 ± 3	[4]
..	Gabbro	SHRIMP zircon U-Pb	222 ± 8	[4]

Table 3: Geochronological data for the Cu–Ni sulphide deposits and mafic rocks in the eastern CAOB.



References

- Şengör AMC, Natal'in BA, Burtman VS (1993) Evolution of the Altaids collage and Paleozoic crustal growth in Eurasia. *Nature* 364: 299-307.
- Jahn BM, Wu FY, Chen B (2000) Granitoids of the Central Asian Orogenic Belt and continental growth in the Phanerozoic. *Transactions of the Royal Society of Edinburgh-Earth Sciences* 91: 181-193.
- Wu FY, Jahn BM, Wilde S, Sun DY (2000) Phanerozoic crustal growth: U-Pb and Sr-Nd isotopic evidence from the granites in northeastern China. *Tectonophysics* 328: 89-113.
- Wu FY, Wilde SA, Sun DY, Zhang GL (2004) Geochronology and petrogenesis of post-orogenic Cu, Ni-bearing mafic-ultramafic intrusions in Jilin, NE China. *J Asian Earth Sci* 23: 791-797.
- Wu FY, Zhao GC, Sun DY, Wilde SA, Zhang GL (2007) The Hulan Group: its role in the evolution of the Central Asian Orogenic Belt of NE China. *J Asian Earth Sci* 30: 542-556.
- Seltmann R, Porter TM (2005) The Porphyry Cu-Au/Mo Deposits of Central Eurasia: 1. Tectonic, Geologic and Metallogenic Setting and Significant Deposits. PGC Publishing, Linden Park.
- Xiao WJ, Windley BF, Hao J, Zhai MG (2003) Accretion leading to collision and the Permian Solonker suture, Inner Mongolia, China: termination of the Central Asian orogenic belt. *Tectonics* 22.
- Xiao WJ, Windley BF, Han CM, Yuan C, Sun M, et al. (2009) End-Permian to mid-Triassic termination of the southern Central Asian Orogenic Belt. *International J Earth Sci* 98: 1189-1217.
- Windley BF, Alexeiev D, Xiao WJ, Kröner A, Badarch G (2007) Tectonic models for accretion of the Central Asian Orogenic Belt. *Journal of the Geological Society London* 164: 31-47.
- Kröner A, Hegner E, Lehmann B, Heinrich J, Wingate MTD, et al. (2008) Palaeozoic arc magmatism in the Central Asian Orogenic Belt of Kazakhstan: SHRIMP zircon ages and whole-rock Nd isotopic systematic. *Journal of Asian Earth Sciences* 32: 2-4.
- He GQ, Li MS, Liu DQ, Zhou RH (1994) Palaeozoic Crustal Evolution and Mineralization in Xinjiang of China. Xinjiang People's Publishing House, Urumqi.
- Charvet J, Shu LS, Laurentt-Charvet S (2007) Paleozoic structural and geodynamic evolution of eastern Tianshan (NW China): welding of the Tarim and Junggar plates. *Episodes* 30: 162-185.
- Jahn BM, Litvinovsky BA, Zandvilevich AN, Reichow M (2009) Peralkaline granitoid magmatism in the Mongolian-Transbaikalian Belt: Evolution, petrogenesis and tectonic significance. *Lithos* 113: 521-539.
- Ye M, Zhang SH, Wu FY (1994) The classification of the Paleozoic tectonic units in the area crossed by Manzhouli-Suifenghe geoscience transect. *Journal of Changchun University Earth Science* 24: 241-245.
- Wu FY, Ye M, Zhang SH (1995) The geodynamic model of the Manzhouli-Suifenghe geoscience transect. *J Earth Sci* 20: 535-539.
- Wilde SA, Zhang XZ, Wu FY (2000) Extension of a newly identified 500 Ma metamorphic terrane in North East China: further U-Pb SHRIMP dating of the Mashan Complex, Heilongjiang Province, China. *Tectonophysics* 328: 115-130.
- JBGMR (Jilin Bureau of Geology and Mineral Resources) (1988) Regional geology of Jilin Province. Geological Publishing House, Beijing, China.
- HJGMR (Heilongjiang Bureau of Geology and Mineral Resources) (1993) Regional geology of Heilongjiang Province. Geological Publishing House, Beijing, China.
- Shi XM, Lan YQ (1985) The metamorphic sequence of Hulan Group, Hongqiling, Jilin province. *Journal of Changchun College of Geology* 4: 39-46.
- Meng FX (1992) The characteristics of zone of progressive metamorphism in argillaceous rock in Hulan Group and its geological significance in the central part of Jilin province. Jilin Nonferrous Metals Geological Exploration Bureau.
- Lv LS, Mao JW, Liu J, Zhang ZH, Xie GQ (2007) Geological Characteristics, Geochronology and Tectonic Settings of Typical

- Magmatic Ni-Cu-(PGE) Sulfide Deposits in the Northern Margin of the North China Craton. *Acta Geoscientica Sinica* 28: 148-166.
22. Fu DB, Chen EZ (1988) Metallogenetic regularities of Cu–Ni sulfide deposits in Jilin province. *Jilin Geology* 2: 124-144.
 23. Qin K (1995) Geological features of magmatic sulfide Cu–Ni deposit at the Hongqiling, Jilin province. *Jilin Geology* 14: 17-30.
 24. Xi AH, Gu LX, Li XJ, Ye SQ, Zhen YC (2005) Discussion on metallogenic epoch of Hongqiling Cu-Ni sulfide deposit, Jilin Province. *Mineral Deposits*.
 25. Foster JG, Lambert DD, Frick LR, Mass R (1996) Re-Os isotopic evidence for genesis of Archaean nickel ores from uncontaminated komatiites. *Nature* 382: 703-706.
 26. Lambert DD, Foster JG, Frick LR, Li CS, Naldrett AJ (1999) Re-Os isotopic systematics of the Voisey bay Cu-Ni-Co magmatic ore system, Labrador, Canada. *Lithos* 47: 69-88.
 27. Shirey SB, Walker RJ (1995) Carius tube digestion for low blank rhenium–osmium analysis. *Analytical Chemistry* 67: 2136-2141.
 28. Stein HJ, Sundblad K, Markey RJ, Morgan MJ (1998) Re–Os ages for Archaean molybdenite and pyrite, Kuittila–Kivisuo, Finland, and Proterozoic molybdenite, Lithuania: testing the chronometer in a metamorphic and metasomatic setting. *Mineralium Deposita* 33: 329-345.
 29. Markey R, Stein JH, Morgan J (1998) Highly precise Re-Os dating for molybdenite using alkaline fusion and NTIMS. *Talanta* 45: 935-946.
 30. Du AD, Wu SQ, Sun DZ, Wang SX, Qu WJ et al. (2004) Preparation and certification of Re-Os dating reference materials: molybdenite HLP and JDC. *Geostandard and Geoanalytical Research* 28: 41-52.
 31. Stein HJ, Markey RJ, Morgan JW, Du AD, Sun YL (1997) Highly precise and accurate Re-Os ages for molybdenite from the East Qinling molybdenium belt, Shaanxi Province, China. *Economic Geology* 92: 827-835.
 32. Smoliar MI, Walker RJ, Morgan JW (1996) Re-Os ages of group IIA, IIIA, IVA and VIB iron meteorites. *Science* 271: 1099-1102.
 33. Ludwig K (2000) *Isoplot/Ex*, version 2.2: A Geochronological Toolkit for Microsoft Excel. Geochronology Center, Special Publication 1a, Berkeley, USA.
 34. Meisel T, Walker RJ, Irving AJ, Lorand JP (2001) Osmium isotopic compositions of mantle xenoliths: a global perspective. *Geochimica et Cosmochimica Acta* 63: 1311-1323.
 35. Barra F, Ruiz J, Mathur R, Tittley S (2003) A Re-Os study of sulfide minerals from the Bagdad porphyry Cu-Mo deposit, northern Arizona, USA. *Mineralium Deposita* 38: 585-596.
 36. Walker RJ, Carlson RW, Shirey SB, Boyd FR (1989) Os, Sr, Nd, and Pb isotope systematics of southern African peridotite xenoliths: implications for the chemical evolution of subcontinental mantle. *Geochimica et Cosmochimica Acta* 53: 1583-1595.
 37. Walker RJ, Morgan JW, Horan MF, Czamanske GK, Krogstad EJ, et al. (1994) Re-Os isotopic evidence for an enriched-mantle source for the Noril'sk-type, ore-bearing intrusions, Siberia. *Geochimica et Cosmochimica Acta* 58: 4179-4197.
 38. Mao JW, Du AD (2002) The 982 Ma Re-Os age of copper-nickel sulfide ores in the Baotan area, Guangxi and its geological significances. *Science in China Series D* 45: 911-920.
 39. Brookes CK, Keays RR, Lambert DD, Frick LR, Nielsen TFD (1999) Re-Os isotope geochemistry of Tertiary picritic and basaltic magmatism of East Greenland: constrains on plume-lithosphere interactions and the genesis of the Platinova reef, Skaergaard intrusion. *Lithos* 47: 107-126.
 40. Naldrett AJ (1997) Key factors in the genesis of Noril'sk, Sudbury, Jinchuan, Voisey's Bay and other world class Cu-Ni-PGE deposits: Implication for exploration. *Australian Journal of Earth Sciences* 44: 283-315.
 41. Yang SH, Zhou MF, Lightfoot PC, Malpas J, QU WJ, et al. (2012) Selective crustal contamination and decoupling of lithophile and chalcophile element isotopes in sulfide-bearing mafic intrusions: An example from the Jingbulake Intrusion, Xinjiang, NW China. *Chemical Geology* 302-303: 106-118.
 42. Lü LS, Mao JW, Li HB, Pirajno F, Zhang ZH, et al. (2011) Pyrrhotite Re–Os and SHRIMP zircon U–Pb dating of the Hongqiling Ni–Cu sulfide deposits in Northeast China. *Ore Geology Reviews* 43: 106-119.
 43. Wu FY, Sun DY, Li HM, Jahn BM, Wilde SA (2002) A-type granites in Northeastern China: age and geochemical constraints on their petrogenesis. *Chemical Geology* 187: 143-173.
 44. Li JY, Gao LM, Sun GH, Li YP (2007) Shuangjingzi middle Triassic syn-collisional crust-derived granite in the east Inner Mongolia and its constraint on the timing of collision between Siberian and Sino-Korean paleo-plates. *Acta Petrologica Sinica* 23: 565-584.
 45. Zhou MF, Leshner CM, Yang ZX, Li JW, Sun M (2004) Geochemistry and petrogenesis of 270 Ma Ni–Cu–(PGE) sulfide-bearing mafic intrusions in the Huangshan district, Eastern Xinjiang, Northwest China: implications for the tectonic evolution of the Central Asian orogenic belt. *Chemical Geology* 209: 233-257.
 46. Lehmann J, Arndt N, Windley BF, Zhou MF, Wang CY, et al. (2007) Field relationships and geochemical constraints on the emplacement of the Jinchuan intrusion and its Ni-Cu-PGE sulfide deposit, Gansu, China. *Economic Geology* 102: 75-94.
 47. Tang ZL, Yan HQ, Jiao JG, Li XH (2006) New classification of magmatic sulfide deposits in China and ore-forming processes of small intrusive bodies. *Mineral Deposita* 25: 1-9.
 48. Wilde SA, Wu FY, Zhao GC, Zhou JB, Sklyarov E (2009) Termination of the eastern Central Asian Orogenic Belt due to onset of Pacific-plate accretion in the latest Triassic-Early Jurassic. In: Lin W, Wang B (eds.), *International Field Excursion and Workshop on Tectonic Evolution and Crustal Structure of the Paleozoic Chinese Tianshan Urumqi, China*.
 49. Lambert DD, Walker RJ, Morgan JW (1994) Re–Os and Sm–Nd isotope geochemistry of the Stillwater complex, Montana: implications for the petrogenesis of the J-M Reef. *Journal of Petrology* 35: 1717-1753.
 50. Ripley EM, Lambert DD, Frick LR (1999) Re-Os, Sm-Nd, and Pb isotopic constraints on mantle and crustal contributions to magmatic sulfide mineralization in the Duluth Complex. *Geochimica et Cosmochimica Acta* 62: 3349-3365.
 51. Walker RJ, Morgan JW, Naldrett AJ, Li C, Fassett JD (1991) Re-Os isotope systematics of Ni–Cu sulfide ores, Sudbury igneous complex: evidence for a major crustal component. *Earth and Planetary Science Letters* 105: 416-429.
 52. Walker RJ, Carlson RW, Shirey SB, Boyd FR (1989) Os, Sr, Nd, and Pb isotope systematics of southern African peridotite xenoliths: implications for the chemical evolution of subcontinental mantle. *Geochimica et Cosmochimica Acta* 53: 1583-1595.
 53. Martin CE (1989) Re-Os isotopic investigation of the Stillwater Complex, Montana. *Earth and Planetary Science Letters* 93: 336-344.
 54. Martin CE (1991) Osmium isotopic characteristics of mantle-derived rocks. *Geochimica et Cosmochimica Acta* 55: 1421-1434.
 55. Frick LR, Lambert DD, Cartwright I (1996) Re-Os dating of metamorphism in the Lewisian Complex, NW Scotland. *Goldschmidt Symposium, Heidelberg, Germany*.
 56. Ravizza G, Turekian KK (1992) The osmium isotopic composition of organic-rich marine sediments. *Earth and Planetary Science Letters* 110: 1-6.